Experimental study of mass transport in PEMFCs: Through plane permeability and molecular diffusivity in GDLs

Prafful Mangal[a], Lalit M. Pant[a,b], Nicholas Carrigy[a], Mark Dumontier[a], Valentin Zingan[a], Sushanta Mitra[b], Marc Secanell[a,*]

[a] *Energy Systems Design Laboratory, Department of Mechanical Engineering, University of Alberta, Edmonton, AB, Canada*
[b] *Micro and Nano-scale Transport Laboratory, Department of Mechanical Engineering, University of Alberta, Edmonton, AB, Canada*

Abstract

An experimental study of convective-diffusive transport in polymer electrolyte fuel cell (PEFCs) porous materials is presented. The study is used to estimate through-plane viscous permeability and effective molecular diffusivity of different gas diffusion layers (GDLs). A diffusion bridge based experimental setup is used for molecular diffusivity measurements, with oxygen and nitrogen flowing across the bridge. The pressure difference across the bridge is adjusted to control convective transport. The oxygen transport across porous media is measured using an oxygen sensor, and experimental data is fitted to a combined Fick's and Darcy's model to estimate effective diffusivity. To measure permeability, a variation of the diffusion bridge is used, where a single gas is forced to go through the GDL. The pressure drop across the GDL is measured, and fitted to Darcy's law to estimate viscous permeability. Through-plane permeability and effective molecular diffusivity are measured for several Toray samples with different polytetrafluoroethylene (PTFE) loading. Results show that permeability varies with PTFE loading between 1.13×10^{-11} - 0.35×10^{-11} m^2 and diffusibility between 0.209 - 0.071. Increase in the PTFE content in GDLs was found to have an adverse effect on permeability and diffusibility.

Keywords: Polymer electrolyte fuel cell; Mass transport; Molecular diffusion; Gas permeability; Gas diffusion media.

1. Introduction

Polymer electrolyte membrane fuel cells (PEFCs) are promising energy conversion devices capable of producing power in the range of watts to kilowatts.

*Corresponding author
Email address: secanell@ualberta.ca (Marc Secanell)

PEFCs can be used in applications such as portable electronics, backup power and automobiles. PEFCs use hydrogen and oxygen as fuel, resulting in water as the only by-product. This results in no local green house gas (GHG) emissions and particulate matter [1]. To make PEFCs competitive in commercial markets, many challenges need to be addressed, and one of them is the manufacturing cost. The cost of a fuel cell can be reduced by either increasing the amount of power produced for the same cell or reducing the amount of platinum per cell [2]. Increased fuel cell performance with the same amount of catalyst or less can be achieved by improving the mass transport properties of different PEFC electrode layers so that the cell can operate at higher current density.

Mass transport in PEFC electrodes takes place in two directions: through-plane, and in-plane. This article is primarily focused on through-plane transport in GDLs. The primary mode of through-plane transport in GDLs is considered to be diffusion [3]. However, it has been shown that convection can also play an important role, especially in serpentine channels [4]. Convection in GDLs is dependent on their permeability. Several studies have measured the through-plane permeability of different types of GDL samples [5–9]. The permeability values of fiber and cloth type GDLs have been reported in the range of 5.7×10^{-12} to 69.4×10^{-12} m^2 [5–7]. The permeability of cloth type GDLs have been reported to be higher than that of fibrous GDLs [6]. Through plane permeability values of carbon paper type GDLs, such as SIGRACET SGL10BA and Toray TGP-H-120, have been found in the range of 8.69×10^{-12} to 31.0×10^{-12} m^2 [8, 9]. The results show wide variation, and also highlight the fact that the permeability of GDLs is highly dependent on manufacturer, porous structure and other additives.

GDLs are often treated with a hydrophobic agent called polytetrafluoroethylene (PTFE) to enhance water transport. The optimum amount of PTFE should repel water to avoid flooding while not inhibiting gas transport significantly. The optimum PTFE content has been reported to be in between 10-20% [10, 11]. The effects of PTFE content on the permeability have been studied by Tamayol et al. [12]. They found that permeability decreases with increasing PTFE content. Ismail et al. [13] also studied the effect of PTFE on through-plane permeability in SIGRACET SGL 10 series samples and measured permeability to vary from 2.72×10^{-11} m^2 at 5% PTFE to 2.19×10^{-11} m^2 at 20% PTFE, with results showing no trend with PTFE content. Due to the limited studies and no consensus in literature, a detailed study on the effect of PTFE on permeability would be worthwhile.

Apart from convection, another phenomena of major interest in gas transport through porous materials is molecular diffusion. Through plane molecular diffusion has been studied experimentally by a number of researchers [14–17]. Techniques such as a diffusion bridge [14], a Loschmidt cell [15, 16] and an electrochemical limiting-current method [17] have been used for effective diffusivity measurements. These studies suggest that the effective diffusivity decreases with

increase in PTFE content [14–17]. The effect of thickness on GDL diffusivity has been found to be almost non-existent [14, 16]. In the micro porous layer (MPL) coated GDLs however, lower thickness resulted in lower diffusivity [14]. The diffusivity has been measured consistently in the order of 10^{-6} m^2/s.

Even though different experimental methods have been developed to measure both permeability or molecular diffusivity, an experimental setup that can measure both values, for the same sample, under the same conditions, has not yet been developed. Furthermore, a setup to study the interplay between convective and diffusive gas transport does not exist. Such experimental setup however is necessary in order to validate the accuracy of advection-convection mass transport models currently used in fuel cell mathematical modeling.

In this article, an experimental technique based on a diffusion bridge is proposed to measure the permeability, and effective molecular diffusivity in the through-plane direction of a porous media. The setup originally proposed by Pant et al. [18] has been extensively modified by introducing a different set of pressure sensors, pressure controllers to control convection, and oxygen sensors. The diffusion measurements are conducted after permeability measurements without disturbing the sample in the diffusion bridge, thereby ensuring both convection and diffusion effects are captured. The experimental data is obtained at steady-state. Therefore, a steady-state advective-diffusive mass transport mathematical model can be used for parameter estimation. The use of a steady-state model simplifies the parameter estimation process which is more complex in the case of transient measurements such as in a Loschmidt cell. The disadvantages of this setup compared to a Loschmidt cell however are that the setup cannot be validated by measuring the bulk diffusivity of a pair of gases and that the experimental equipment is more complex.

Section 2 discusses the experimental setup, samples tested, and experimental conditions. Section 3 focuses on the theoretical models used to interpret the data, their assumptions and the implementation. Section 4 discusses the results for the tested samples and their validation with the literature.

2. Materials and Methods

This section explains the experimental methods used for the transport property measurements and the description of the setup for permeability and effective molecular diffusivity.

2.1. Mercury Intrusion Porosimeter

The porosity of the samples was measured by mercury intrusion porosimeter. Porosimetry tests were performed using a PoreMaster 33 Mercury Porosimeter (Quantachrome Instruments). 20 cm^2 of GDL sample was used for each test,

cut into strips measuring 2.24 cm by 0.56 cm.

To perform the intrusion test, the sample is placed inside the bulb of a glass penetrometer cell with 0.5 cc stem volume. The penetrometer cell is evacuated to an absolute pressure of 26.91 Pa (0.0039 psi) and then further evacuated for 30 minutes. The cell is filled with mercury and the mercury is then pressurized, up to a maximum pressure of 2.277×10^8 Pa (33000 psi). The change in volume of mercury is measured as the pressure increases.

Porosity of each sample is calculated using the following equation:

$$\epsilon_o = \frac{V_{pore}}{V_{total}} \tag{1}$$

where ϵ_o is porosity, V_{pore} is the intruded pore volume and V_{total} is the total volume of the sample (both solid and void-space), V_{pore} is measured directly from the mercury intrusion test. Total volume of the sample is calculated by measuring the outer dimensions of the sample using a digital micrometer (Mitutoyo, Japan, Absolute Digimatic Micrometer, Order no: 227-201).

The logarithmic pore size distribution, $\frac{\mathrm{D}X}{\mathrm{D}(\ln(r))}$, for a given pressure p_i normalized with respect to total sample volume, is calculated using the following equation:

$$\frac{\mathrm{D}X}{\mathrm{D}(\ln(r))} = \frac{(V_i - V_{i-1})/V_{pore}}{\ln(p_i) - \ln(p_{i-1})} \tag{2}$$

where X is the cumulative pore volume fraction, V_i is the absolute intruded volume measured up to pressure p_i, and V_{pore} is the total measured intruded volume, $\frac{\mathrm{D}X}{\mathrm{D}(\ln(r))}$ is plotted with respect to pore radius to produce the pore size distribution curve for each sample.

The pore radius is estimated using the Washburn equation,

$$r = -2\frac{\gamma\cos(\theta)}{p} \tag{3}$$

where p is the applied pressure, r is the pore radius, γ is the surface tension of mercury and θ is the contact angle between the mercury and the sample material. For the tests of the GDL, samples γ was taken as 480 dyne/cm^{-1} and θ as 140°.

Table 1 shows the measured thickness and porosity of the GDL samples under study. The standard deviation from multiple thickness readings on the sheet and its impact on porosity prediction is also shown. Figure 1 shows logarithmic pore size distribution and cumulative pore volume fraction distribution for Toray090 samples with different PTFE content. The higher PTFE content reduces the porosity and the effective pore diameter due to the penetration of PTFE in the available pores as shown in Table 1. Also, based

on MIP data, the porosity with varying PTFE content is linearly fitted as, $\epsilon_o = 0.835 - 0.0074 \times (PTFE\%)$. This expression is valid only for PTFE content between 10 - 40%.

2.2. Diffusion bridge

A flow channel is machined into two acrylic plates to form the flow channels of the diffusion bridge. The two plates are assembled together with the gas diffusion layer in between them completing the diffusion bridge. Figure 2 shows the exploded view of the diffusion bridge. Two rectangular channels of length 150 mm and cross section area of 15×2 mm^2 are machined in the plates. The channel lengths are designed to make sure that the gas flow field is fully developed prior to its exposure to the porous media.

In order to test a GDL, a sample of dimension 20 x 25 mm^2 is prepared by cutting the sample from a master sheet using an X-Acto knife. Three samples of equal dimensions are stacked upon each other in all the experiments. The prepared samples are shown in Figure 3. The sample is laminated (HeatSeal H220 laminator) in a 3 mil lamination sheet, and a hole of diameter 9.5 mm is punched in the center of the lamination sheet to allow the gas to pass through the porous media. The thickness of the layers are measured using a micrometer (Mitutoyo, Japan) at a load of 0.5 N. The layers compress during the lamination. The amount of compression is estimated by measuring the thickness of sample before and after lamination, and calculated to be less than 5% for Toray 090 samples. The change in porosity due to compression is estimated to be less than 1%, therefore no correction for compression is applied.

The two plates are aligned and assembled together using bolts that are tightened in a cross cyclic manner to create a uniform compression. The bolts were tightened using a torque wrench. A torque value of 10 N-m was found sufficient for assembly without damaging or bending the acrylic plates. A 10 mil silicon gasket is placed around all the edges of the diffusion bridge to prevent any leakage. The bridge was pressurized at 40 psig for 12 hours to detect leakage and no leakage was observed.

2.3. Through-plane permeability setup

The schematic of the permeability measurement setup is shown in Figure 4. The setup is a variation of the diffusion bridge technique. The diffusion bridge contains two channels, each with four connection ports. One end of the high pressure channel is connected to a mass flow controller, and the low pressure channel is open to atmosphere at one port. The other ports are closed in such a way that the flow is forced to go through the GDL sample.

Compressed nitrogen (Praxair, UHP 5.0) is decompressed using a pressure regulator. Nitrogen at 50 psig is then made available to the mass flow controller. The mass flow controller (Cole-Parmer, model: RK-32907-69, range: 0-5 lpm) is used to control the flow rates. The mass flow controller is connected to a computer via an RS-232 communication port. While going through the porous media, the gas undergoes certain pressure drop. This pressure drop is measured by a differential pressure transducer (OMEGA, Model: -MMDDB001BIV10H2A0T1A2) connected across the channels. The data from the pressure transducer is read via a data acquisition card (National Instruments USB 6221). LabWindows/CVI is used to communicate with the mass flow controller and log data from the mass flow controller and pressure transducer. The data is logged for 5 minutes (60 readings) for all flow rates, and all the readings are used to obtain the average pressure drop. Based on all the readings, the standard deviation is found to be less than 3%.

2.4. Through-plane diffusivity setup

The schematic of effective diffusivity measurement setup is given in Figure 5. The inlet of each channel in the diffusion bridge is connected to a different gas cylinder, e.g., one containing oxygen and an other nitrogen. The two compressed gases are decompressed before passing through the mass flow controllers. Two mass flow controllers (Cole-Parmer, model: RK-32907-69, range: 0 - 5 lpm) are used to control the flow rate of gas in the channels. The outlet of the nitrogen channel is connected to a back pressure controller (Cole-Parmer, model: RK-00307OX, range: 0 - 100 psig) that is used to control the static pressure of the system. The oxygen channel outlet is connected to a differential pressure controller (Cole-Parmer, model: RK-00307TX, range: 0 - 500 Pa) which controls the static pressure difference between the two gas channels using a differential pressure gauge connected to each channel. The differential pressure controller is used to control the pressure difference across the channels, thereby controlling the convective transport. Oxygen levels are measured at the outlet of the nitrogen channel downstream of the back pressure controller using a NEOFOX oxygen sensor (Ocean Optics, Model: FOSPOR-600-32MM, range: 0 - 10% in gas). The fibre core diameter of the sensor is 1mm, and outer diameter is 1.587mm. The response time of the sensor is less than 60 seconds. The sensor is factory calibrated for a range of 0-10 % O_2 and temperature 0-80°C. The range of temperature covered for calibration ensures the consistent readings during day to day temperature fluctuations. The calibration file is uploaded in the NEOFOX software before experiments are started. Single point calibration is performed in-house, after the multi-point calibration file is uploaded. Pure nitrogen gas (UHP 5.0) is exposed to the sensor and the reading is recorded as zero. Single point calibration is done every time before the experiments are started.

The extent of convective transport is controlled by modifying the oxygen gas channel pressure. The oxygen channel is set at higher pressure than the nitrogen channel in order to enhance oxygen mass transport through the porous media

via convective transport. To control the differential pressure between channels, a differential pressure controller is installed in the oxygen channel. Oxygen and nitrogen channel pressure are obtained at the channel. The absolute pressure in the setup is controlled by a back pressure controller in the nitrogen channel.

Mass flow controllers and pressure controllers are connected to a computer via RS-232 communication port. The data from pressure transducer is read via a data acquisition card. LabWindows/CVI is used for data logging and storing the data in a Excel file. Data for every set-point is logged, at a rate of one reading every 5 seconds, for 5 minutes. The software provided by the NEOFOX sensors also stores the detected oxygen mole fraction with time, temperature and pressure in a CVS file every 2 seconds. For every differential pressure, 150 readings for oxygen mole fraction are logged approximately. The average of the last eighty readings is reported. The real time is also recorded simultaneously from both CVI and NEOFOX software to map the data accurately for oxygen mole fraction to its corresponding differential pressure. The data from Excel and CVS files are merged manually and used for further analysis.

2.5. Experimental conditions

For permeability experiments, the mass flow rate of nitrogen gas is varied from 0-2 liters per minute (lpm) in 10 even intervals for a GDL sample. The 'zeroth interval', which corresponds to zero flow rate, is run for five minutes to estimate the offset of the pressure transducer. The offset is eliminated from the average readings at non zero flow rates. The average standard deviation for the selected flow rates from the MFC and pressure transducer is observed to be less than 3.0% of the average value.

For through-plane diffusivity experiments, the mass flow rate of both gases is set at 1 liters per minute (lpm). High flow rates are used to ensure the oxygen is quickly swept away in the nitrogen channel and the effects of diffusive boundary layer are minimized. The back pressure of the system is maintained at a pressure of 10 psig unless otherwise stated. The pressure difference between the two channels is varied from 2 - 10 Pa in 5 even intervals. The low differential pressures are selected to ensure the oxygen concentrations are within the measuring range of the oxygen sensor. The differential pressure controller's pressure is obtained from averaging the last 40 readings at each setpoint. As shown in Figure 8, oscillations are observed in the controller. The standard deviation from 40 consecutive readings is less than 2 Pa for each setpoint. Oxygen mole fraction is recorded at every pressure differential. The temperature of the system in both cases is ambient.

2.6. Testing Protocol

Unless otherwise specified, the GDL samples are tested with three layers stacked over each other. The aperture diameter is fixed as 9.5mm. The results shown in section 4 are the average of three specimens cut from the same master

sheet in random directions. The standard deviation corresponds to sample-to-sample variation in transport properties cut from same master sheet. Hence, results consist of errors from experimental equipment, directionality of fibers, and sample-to-sample effects.

3. Theory and Data Analysis

3.1. Mathematical models

3.1.1. Governing equation for through-plane permeability

Darcy's law is commonly used to estimate the permeability of a porous media. Mathematically it is defined as [19, pp. 148]

$$\nabla p = -\frac{\eta}{B_v}\mathbf{v}, \tag{4}$$

where ∇p is the pressure gradient across porous media, $\mathbf{v}$ is the velocity, η is the dynamic viscosity and B_v is the porous media viscous permeability.

Darcy's law accurately quantifies porous media permeability for Stokes flow, also known as creep flow. At high flow rates, the fluid experiences various accelerations and deaccelerations as it flows through the porous media [5]. This effect, known as Forcheimer effect, is considered to be negligible for sufficiently low velocities but can play a significant role when the velocities are high. In such cases, Darcy's law can be extended in order to obtain the Forcheimer equation, which in one dimension is given by [5]

$$\frac{\mathrm{d}p}{\mathrm{d}x} = -\frac{\eta}{B_v}v - \frac{\rho}{B_l}v^2, \tag{5}$$

where x is the direction following the flow direction and B_l is known as the inertial permeability. Assuming the fluid is an ideal gas and replacing velocity with molar flux, equation (5) can be written as:

$$\frac{\mathrm{d}p}{\mathrm{d}x} = -\frac{RT}{p}\left(\frac{\eta}{B_v}N + \frac{M}{B_l}N^2\right). \tag{6}$$

In the absence of a chemical reaction, the molar flux is constant. Then, integrating equation (6) from 0 to L and p_1 to p_2, the compressible form of the Darcy-Forcheimer equation becomes

$$\frac{p_1^2 - p_2^2}{2RTL} = \frac{\eta}{B_v}N + \frac{M}{B_l}N^2, \tag{7}$$

where p_1 and p_2 are the pressures of the gas at the inlet and outlet of the porous media respectively, T is the temperature, R is the gas constant, L is the thickness of the sample, M is the molecular weight and N is the molar flux of the gas. In terms of mass flux, n, the Darcy-Forcheimer equation can be written as,

$$\frac{p_1^2 - p_2^2}{2RTL/M} = \frac{\eta}{B_v} n + \frac{1}{B_l} n^2. \tag{8}$$

3.1.2. Governing equations for through-plane diffusivity

Fick's first law is commonly used for analyzing the transport of binary mixtures and of a solute in an infinitely dilute mixture. Mathematically, it is defined in a porous media as [19, pp. 515]

$$\mathbf{n}_i^D = -D_{ij}^{eff} \nabla \rho_i, \tag{9}$$

where $\mathbf{n}_i^D$ is the superficial mass flux of species i, i.e., $n_i^D = \epsilon\, n_i$, ρ_i is the mass density of species i, and $D_{ij}^{eff} = \dfrac{\epsilon}{\tau}\, D_{ij}$, where ϵ is the porosity, and τ is the tortuosity of the porous media. The ratio of $\dfrac{D_{ij}^{eff}}{D_{ij}}$ is defined as the diffusibility of the porous media. Equation (9) can also be written as

$$\rho_i(\mathbf{v}_i - \mathbf{v}) = -D_{ij}^{eff} \nabla \rho_i, \tag{10}$$

where $\mathbf{v}_i$ is the velocity of species i, and $\mathbf{v}$ is the average mass velocity, defined as

$$\mathbf{v} = \frac{\Sigma \rho_i \mathbf{v}_i}{\Sigma \rho_i} = \frac{\Sigma \rho_i \mathbf{v}_i}{\rho_m} = \Sigma \omega_i \mathbf{v}_i. \tag{11}$$

Equation (10) can be simplified to

$$\mathbf{n}_i = \rho_i \mathbf{v}_i = \rho_i \mathbf{v} - D_{ij}^{eff} \nabla \rho_i, \tag{12}$$

where $\mathbf{n}_i$ is the mass flux of species i.

Assuming one dimensional flow, and replacing i and j species with oxygen and nitrogen respectively, equation (12) can be rewritten as:

$$\mathbf{n}_{O_2} = \rho_{O_2} \mathbf{v}_{O_2} = \rho_{O_2} \mathbf{v} - D_{O_2,N_2}^{eff} \frac{d\rho_{O_2}}{dx} = \rho_{O_2} \frac{n_m}{\rho_m} - D_{O_2,N_2}^{eff} \frac{d\rho_{O_2}}{dx}, \tag{13}$$

where $\mathbf{n}_{O_2}$ is the mass flux of oxygen, n_m, and ρ_m are the mass flux and density of the mixture, respectively.

In the absence of a chemical reaction, the mass flux of oxygen is constant, and the divergence of $\mathbf{n}_{O_2}$ is zero, i.e.

$$\nabla \cdot \mathbf{n}_{O_2} = 0 \Rightarrow \frac{dn_{O_2}}{dx} = 0. \tag{14}$$

Similarly, mass flux of the mixture is constant:

$$\frac{dn_m}{dx} = 0, \tag{15}$$

Using Darcy's law for the mixture of species:

$$v = -\frac{B_v}{\eta}\frac{dp_m}{dx} \Rightarrow n_m = -\frac{B_v}{\eta}\rho_m\frac{dp_m}{dx}, \tag{16}$$

where B_v is the viscous permeability of the porous media, p_m is the mixture pressure, and η is the dynamic viscosity of the gas mixture. The mixture viscosity, η, is approximated as the average of the viscosity of oxygen and nitrogen, $\eta = \frac{\eta_{O_2} + \eta_{N_2}}{2}$. Since the velocity through the porous media is small for the diffusion experiments, the Forcheimer term is neglected.

Equations (13) - (16) are the governing equations for the fluid in the porous media. They are used to estimate oxygen and mixture fluxes, oxygen mass density and mixture pressure, i.e., n_{O_2}, n_m, ρ_{O_2}, and p_m respectively. Nitrogen mass fraction and mass flux can be estimated at post-processing using ρ_{N_2} = ρ_m - ρ_{O_2} and $n_{N_2} = n_m$ - n_{O_2}.

3.2. Data analysis

In the permeability experiments, the mass flow rate and pressure drop are obtained experimentally. The inlet velocity is obtained using the aperture diameter of the porous media. The molar flux is obtained using $N = \frac{pv}{RT}$, where v is the inlet velocity and p is the inlet pressure. Then, the experimental data is fit to equation (7) using MATLAB to extract transport parameters, i.e., B_v and B_l. The function `fittype` is used for fitting. `fittype` uses a least squares regression technique to minimize the residual. The coefficient of regression for all the fittings is found to be greater or equal to 0.99.

In the effective diffusivity experiments, the oxygen molar fraction, $x_{O_2}^{out}$, and the pressure difference between channels are recorded directly. In order to estimate the experimental oxygen mass flux across the porous media, $n_{O_2,exp}$, first, the molar flux in the nitrogen gas channel and the molar flux across the porous media are calculated. The molar flux in the nitrogen gas channel is given by

$$N_{Ch} = \frac{\rho_{N_2}\dot{V}}{M_{N_2}} \tag{17}$$

where ρ_{N_2} is the density of nitrogen at 10 psig and $\dot{V}$ is the volume flow rate set by mass flow controller. The molar flux through the porous media is calculated as

$$N_p = \frac{p}{RT}Av^*, \tag{18}$$

where p is the pressure in the oxygen channel, i.e. p_{O_2}, A is the cross-sectional area of the aperture in the GDL sample, and v^* is the superficial molar average

gas velocity in porous media. Note also that $N_{Ch} >> N_p$.

To calculate the molar average velocity though the porous media, v^*, the mass average velocity is first calculated as

$$v = \frac{B_v}{\eta}\frac{\Delta p}{L}. \tag{19}$$

where Δp is the pressure difference between channels and B_v is the GDL permeability. Then, the molar average velocity is calculated using [19, pp. 535]:

$$v^* = v + \Sigma x_i(v_i - v) \tag{20}$$

assuming $x_{O_2} = x_{N_2} = 0.5$. Note that the difference between molar and mass average velocities is less than 1% for the worst case scenario, i.e. Toray 090 (10% PTFE) with a $\Delta P = 10$ Pa.

Finally, the experimental mass flux across the porous media, $n_{O_2,exp}$, is estimated as,

$$n_{O_2,exp} = x_{O_2}^{out}\frac{N_p + N_{Ch}}{A}M_{O_2} \tag{21}$$

Equations (13), (14), (15), and (16) are used to estimate n_{O_2}, n_m, ρ_{O_2}, and p_m using the permeability value, B_v, from the through-plane permeability experiments. The equations are solved using the MATLAB `bvp4c` solver. The solver requires four boundary conditions to solve the system of equations. In this case the following are used: ρ_{O_2} =2.405 (density of oxygen at 10 psig gauge pressure) and $p_m = p_{O_2}$ at $x = 0$, and ρ_{O_2} =0 and $p_m = p_{N_2}$ at $x = L$. The maximum oxygen mole fraction in the whole set of experiments has been measured less than 0.04, and is further diluted due to the entrainment of nitrogen. Therefore, as a boundary condition, the oxygen mass density is approximated as zero at $x = L$. Simulations at different pressures with different values of the effective oxygen diffusion coefficient, $D^{eff}_{O_2,N_2}$, are performed and a residual function defined as the square of the difference between the experimental and numerical mass fluxes at different pressures is computed using

$$R(p) = \sum_{i=1}^{5}(n_{O_2,exp}(\Delta p_i) - n_{O_2,num}(\Delta p_i, D^{eff}_{O_2,N_2}))^2. \tag{22}$$

The estimated effective diffusion coefficient, $D^{eff,*}_{O_2,N_2}$, is the value that minimizes the residual function.

4. Results and discussion

4.1. Through-plane permeability

Various commercial GDLs shown in Table 1 were tested, and properties were estimated using method discussed in previous section. This section discusses the experimental results, uncertainly analysis and the validation of the results.

Test variability. The reliability of the setup is determined by assembling a diffusion bridge with a Toray 090 (10% PTFE) sample and running the same experiment three times without opening/closing the diffusion bridge. The pressure gradient versus velocity data is obtained from the setup for all three sets of readings. The three values are 0.95×10^{-11}, 0.94×10^{-11} and 0.94×10^{-11} m^2, thus the standard deviation in the viscous permeability results is estimated as 0.64%.

Variation within aperture diameter. The aperture diameter punched in the lamination sheet was varied to study the effects on the permeability results. Three Toray 090 (0% PTFE) layers were stacked in each case. Four different aperture diameters were punched in the lamination sheet. The permeability for samples with aperture diameter 4.69, 6.8, 7.8, and 9.5 mm was estimated as 1.22×10^{-11}, 0.90×10^{-11}, 1.01×10^{-11}, and 1.39×10^{-11} m^2, respectively. The standard deviation of the viscous permeability for diameters larger than 4mm is obtained as 19.47%. The standard deviation for sample-to-sample variation of Toray 090 (0% PTFE) is obtained as 6.25% (see Table 2). However, for a 95% confidence interval, a Student's t-test shows that the results obtained with different aperture diameter are not significantly different from results shown in Table 2. Therefore, the difference from aperture diameters is within sample-to-sample variability. The discrepancies between results obtained with different aperture radii, and shown in Table 2, are due to the use of samples from different master sheets. The aperture diameter was fixed at 9.5 mm for the results discussed in this article ensuring a sufficiently large representative elementary volume is used to reflect the average geometric properties of the porous media.

Variation with number of layers. The number of layers of a SGL 34BA were varied to study the effects on the permeability results. A SGL 34BA was tested with single, two, three and four layers stacked over each other. The aperture diameter was fixed at 9.5mm. The permeability for single, two, three, and four layers is estimated as $(1.07\pm0.32)\times10^{-11}$, $(1.30\pm0.24)\times10^{-11}$, $(1.09\pm0.12)\times10^{-11}$, and $(1.37\pm0.44)\times10^{-11}$ m^2, respectively. The standard deviation is obtained by testing 3 replicates of each stack. A Student's t-test is performed to compare the results obtained for different number of layers. For 95% confidence interval, the results were not found to be significantly different. The three layers showed the best repeatability, hence three layers were stacked for all the GDL samples tested in this study.

Validation. SGL 34BA permeability was measured and compared to several data values available in the literature. The obtained results are in agreement with previous data. The difference in results between Table 2 and the results obtained for different number of layers is due to the use of different master sheets. The difference in the results corresponds to differences between master sheets.

4.1.1. Effect of PTFE on through-plane permeability

The effect of PTFE was studied by testing Toray 090 samples with 0, 10, 20 and 40% PTFE. Compressible form of Darcy - Forcheimer equation (equation (7)) is used to estimate the permeability. Figure 6 shows the inlet pressure vs molar flux curves for the Toray 090 samples. The inlet pressure increases with higher PTFE content at the same velocity. Table 2 shows the permeability results for the tested samples. The standard deviation was obtained by testing three replicates of the same sample cut from the same master sheet. The results are compared with literature, and found in good agreement. The slight difference between the results is due to sample variability, and errors influenced by sample preparation. Results show that permeability decreases with increasing content of PTFE except for Toray 090 (10% PTFE) which showed higher permeability than untreated sample. The small amount of PTFE does not seem to vary the geometric properties significantly. The permeability decreases with high PTFE content due to the spread of PTFE binders over the intersection of fibers thereby reducing pore size and porosity.

The permeability for non-overlapping fibre structure is often predicted by Carman-Kozeny equation [20], i.e.

$$K = \frac{d_f^2 \epsilon^3}{16 K_{CK} (1-\epsilon)^2}, \tag{23}$$

where d_f is the fiber diameter, ϵ is the porosity and K_{CK} is known as the Carman-Kozeny constant which is considered a fitting parameter. The permeability results for Toray 090 (10, 20 and 40% PTFE) are fitted in equation (23) to extract Carman-Kozeny constant, K_{CK}. The fiber diameter for Toray 090 samples is used as 9.2μm [5]. The constant is estimated as 3.35$\pm$0.31. Figure 7 shows the comparison of Carman-Kozeny equation with the experimental data. The prediction of permeability is accurate for low PTFE content samples but discrepancies occur at high PTFE content. The Carman-Kozeny model was developed to estimate the permeability for materials made of cylindrical fibres [20]. At high PTFE content, the fibers deviate from their cylindrical shapes and as a result the model does not provide a good fit to the data. The Carman-Kozeny equation therefore appears to only be able to provide only a rough estimate of the actual permeability of the sample.

4.2. Through-plane effective diffusivity

A diffusion bridge is created between the pair of oxygen and nitrogen gas. Various commercial GDL samples are tested, viz: Toray 090 with 0, 10, 20 and 40% PTFE loadings.

4.2.1. Error analysis

Test variability. The reliability of the setup is determined by assembling a diffusion bridge with a Toray 090 (10% PTFE) sample and running the same experiment five times without disturbing the diffusion bridge chip. The oxygen

molar flux versus differential pressure data is obtained from the setup for all five sets of readings, and the diffusibility is estimated as discussed in section 3. The standard deviation for diffusibility is estimated as 13.11%.

Figure 8 shows the average and actual differential pressure, and oxygen concentration readings for a Toray 090 (10% PTFE) sample. The average values in the figure are estimated by averaging the last sixty measured readings for oxygen sensor, and all the readings from differential pressure controller. Due to the different rate of data logging from LabWindows/CVI and NEOFOX software, only sixty readings for oxygen sensor are shown in figure 8. Fluctuations in the differential pressure controller are observed. These fluctuations result in small fluctuations in the oxygen concentration. The magnitude and value of the pressure oscillations were confirmed with a second pressure transducer. The fluctuations in a GDL sample are observed due to its high permeability. GDLs with MPL do not show such fluctuations. As shown in the figures, the fluctuations are small compared to the changes due to differential pressure setpoints. Even with the observed fluctuations, the results were found to be repeatable.

Variation with channel flow rate. The boundary layer effects are studied by measuring diffusion at different flow rates without disturbing the diffusion bridge. Sample Toray 090 (10% PTFE) is tested at 0.5, 1, 1.5 and 2 lpm, and diffusibility is estimated. The diffusibility values at 0.5, 1, 1.5 and 2 lpm are estimated as 0.183 ± 0.009, 0.183 ± 0.024, 0.197 ± 0.004, and 0.200 ± 0.005, respectively . The standard deviation is obtained by repeating the experiment five times at each flow rate without disturbing the diffusion bridge. A Student's t-test is performed to compare the results obtained for different flow rates. For 95% confidence interval, results were not found to be significantly different.

4.2.2. Validation studies

Effect of absolute pressure. Kinetic theory of gases predicts that the product of absolute pressure and molecular diffusivity is constant. Mathematically,

$$PD_{bulk} = constant. \tag{24}$$

The experimental method is verified by changing the absolute pressure of the diffusion bridge in the nitrogen channel to 10, 15 and 20 psig using a back pressure controller for a Toray 090 (10% PTFE) sample. Diffusibility is a geometric property of porous media and it should not vary with the absolute pressure. Experimentally, the diffusibilities at different pressures were obtained as 0.183 ± 0.024, 0.173 ± 0.005, and 0.176 ± 0.013 at 10, 15 and 20 psig, respectively. The standard deviation is obtained by repeating the experiment 5 times at each back pressure. For 95% confidence interval, a Student's t-test suggests that diffusibility results at 10, 15 and 20 psig are not significantly different from each other.

Different pair of gases. The diffusibility is a geometric property of porous media, hence not expected to vary with a pair of experimental gases chosen. Sample Toray 090 (10% PTFE) is tested with two pair of gases i.e., $N_2 - O_2$ and $Ar - O_2$. For each pair of gases, experiments are repeated 5 times. The bulk diffusion coefficient for $N_2 - O_2$ and $Ar - O_2$ at ambient conditions is used as 2.065×10^{-5} and 1.95×10^{-5} m^2/s respectively. Diffusibility for $N_2 - O_2$ and $Ar - O_2$ is estimated as 0.183±0.024 and 0.183±0.009, respectively. For 95% confidence interval, a Student's t-test justifies that diffusibilities are not significantly different from each other.

A similar study was performed with $He - O_2$. The diffusibility results for $He - O_2$ were found to be significantly different, which was unexpected. Further work is necessary to understand this effect.

4.2.3. Effect of PTFE on through-plane diffusivity

The effect of PTFE on diffusivity is studied by testing Toray 090 samples with 0, 10, 20 and 40% PTFE. Diffusibility is estimated using Fick's and Darcy's model (equation (13), (14), (15), and (16)). For GDLs, Knudsen diffusivity is assumed to be zero, as shown by Carrigy et al. [21]. The permeability values were used from the permeability measurements. Figure 9 shows the oxygen molar flux vs differential pressure curves obtained experimentally and from fitting Fick's and Darcy's model for best fit of diffusibility. For all four materials, Fick's and Darcy's model were able to closely predict the experimental results. The flux was found to decrease with PTFE content at zero differential pressure suggesting that the effective diffusivity decreases with PTFE content. At non-zero differential pressures, oxygen molar flux decreases as the PTFE content increases. As discussed in section 4.1, high PTFE content decreases the permeability, hence the molar flux due to convection also decreases.

Table 3 shows the diffusibility results, and a comparison to previous literature data. Though the tested samples are Toray 090, results are compared with Toray 060 and Toray 120. The Toray 060, 090 and 120 are known to have similar porosity, hence comparable transport properties. The samples differ only in physical properties such as thickness and tensile strength. The results were found in good agreement with literature. Note that the experimental setup used here is completely different than any of the previous methods used thereby validating previous results. The diffusibility was estimated to decrease with higher PTFE content. As already discussed, PTFE binders block the pores of the porous media, thereby reducing its size.

To predict the diffusibility in porous media, various models have been proposed. A Bruggeman type correlation [22] is widely accepted. Mathematically, the empirical correlation of the model is defined as:

$$D_{eff}/D_{bulk} = \epsilon^a \tag{25}$$

where a is considered a fitting parameter. In the case of Bruggeman, a is usually taken as 1.5. The diffusibility results are fitted in equation (25) in MATLAB. The function `lsqcurvefit` is used for fitting. Figure 10 shows the fitting of the experimental data with the model. The fitting parameter a in Bruggeman correlation is estimated as 5.63±0.82. Note that the common value of 1.5 in Bruggeman correlation is not suitable as previously pointed out by different researchers [14–17] using different experimental apparatus.

4.2.4. Oxygen flux distribution in a GDL sample

Using the Darcy's and Fick's mathematical model, and the obtained transport parameters, oxygen flux distribution is studied in a Toray 090 (10% PTFE) sample. The thickness, permeability and effective molecular diffusivity of the sample was measured as 869μm, 0.91×10^{-11} m^2 and 0.25×10^{-5} m^2/s, respectively. Figure 11 shows the oxygen density curves across the sample at various differential pressures. At zero pressure difference, oxygen density decreases linearly. At non zero pressure difference, the density profiles are non-linear due to the additional flux via convection. The oxygen mole fraction is measured to be less than 2% in the nitrogen channel and quickly diluted due to the entrainment by the nitrogen flow, hence the oxygen partial pressure is approximated as zero as a boundary condition. Therefore, oxygen density and convective flux is zero at the outlet of the porous media.

Figure 12 and 13 show the oxygen flux distribution via convection and diffusion, respectively. At zero differential pressure, convective flux is zero, hence total flux corresponds to pure diffusive flux. At the inlet of the porous media, diffusive flux dominates the convection for differential pressures less than 6 Pa. The diffusive flux contribution decreases from 79% to 31% as pressure difference increases from 2 to 10 Pa. The total oxygen flux increases from 0.0134 to 0.006 kg/s m^2 for pressure difference increasing from 0 to 10 Pa. At any point in the porous media, the total oxygen flux is constant. Due to the comparable contribution from both convective and diffusive flux, the experimental conditions chosen are suitable to study a coupled advection-diffusion.

5. Conclusions

A diffusion bridge based experimental setup is proposed to study advection-diffusion in fuel cell GDLs and measure effective transport properties of porous media, i.e. permeability, and molecular diffusivity in the through-plane direction. The effect of PTFE on transport properties is studied by testing Toray 090 samples with 0, 10, 20 and 40% PTFE.

Permeability is estimated by measuring the pressure drop across porous media at various flow rates. The effective molecular diffusivity is measured by introducing nitrogen and oxygen in the channels of the diffusion bridge. The absolute pressure of nitrogen and pressure difference between oxygen and nitrogen is controlled by pressure controllers. The oxygen concentration at various

pressure differentials is measured in the nitrogen channel using an oxygen sensor.

A one dimensional Fick's and Darcy's model is used to fit to experimental data. For four different samples, two different gases, and at different pressures, the model is capable of closely predicting oxygen flux. Thereby, for binary mixtures, the combined Fick's and Darcy's model is suitable to analyze advection-diffusion transport in porous media.

Using the one dimensional models, permeability and diffusivity are estimated. The permeability of Toray 090 samples is obtained in the range of 1.13×10^{-11} - 0.35×10^{-11} m^2, and found to decrease with PTFE content. The diffusibility for GDL samples is measured in the range of 0.248 - 0.086.

The measured parameters are used to fit in the models to predict transport properties. Carman-Kozeny model is used to fit for parameter K_{CK} to predict the permeability. Bruggeman model is fitted to the diffusibility results to predict the diffusion coefficient in the through-plane direction. The parameters obtained using the model should be helpful to study the gas behaviour in porous media using 2D and 3D simulations.

In this article, the proposed experimental setup is used to study advection-diffusion of binary mixtures in GDLs. In fuel cells are usually operated using a multi-component gas mixture. Further, even though Knudsen transport effects can be ignored in GDLs, see reference [21], this is not the case for MPLs and CLs. Using the proposed setup, it should also be possible to study both of these effects. Results for multi-component mass transport and MPLs and CLs where Knudsen effects are important could be used to analyze the suitability of the different multi-component mass transport models currently available in the literature [23].

6. Acknowledgements

The authors would also like to thank the Natural Sciences and Engineering Research Council of Canada (NSERC), the Canada Foundation for Innovation (CFI), and the Government of Alberta Small Equipment Grant Program for financial support. The authors would also like to thank the Automotive Fuel Cell Cooperation (AFCC) for providing some of the GDL samples used in this study.

References

[1] F. Wagner, B. Lakshmanan, M. Mathias, Electrochemistry and the future of the automobile, Journal of Physical Chemistry Letters 1 (14) (2010) 2204–2219.

[2] J. Wishart, Z. Dong, M. Secanell, Optimization of a PEM fuel cell system for low-speed hybrid electric vehicles, in: ASME 2006 International Design Engineering Technical Conferences & Computers and Information in Engineering Conference, Philadelphia, Pennsylvania, USA, 2006.

[3] J. Feser, A. Prasad, S. Advani, Experimental characterization of in-plane permeability of gas diffusion layers, Journal of power sources 162.

[4] J. Pharoah, On the permeability of gas diffusion media used in PEM fuel cells, Journal of Power Sources 144 (2005) 7782.

[5] J. T. Gostick, M. W. Fowler, M. D. Pritzker, M. A. Ioannidis, L. M. Behra, In-plane and through-plane gas permeability of carbon fiber electrode backing layers, Journal of Power Sources 162 (1) (2006) 228–238.

[6] I. Hussaini, C. Wang, Measurement of relative permeability of fuel cell diffusion media, Journal of Power Sources 195 (12) (2010) 3830–3840.

[7] V. Gurau, M. J. Bluemle, E. S. De Castro, Y.-M. Tsou, T. A. Zawodzinski Jr, J. A. Mann Jr, Characterization of transport properties in gas diffusion layers for proton exchange membrane fuel cells: 2. Absolute permeability, Journal of power sources 165 (2) (2007) 793–802.

[8] M. V. Williams, E. Begg, L. Bonville, H. R. Kunz, J. M. Fenton, Characterization of gas diffusion layers for PEMFC, Journal of the Electrochemical Society 151 (8) (2004) A1173–A1180.

[9] J. Ihonen, M. Mikkola, G. Lindbergh, Flooding of gas diffusion backing in PEFCs physical and electrochemical characterization, Journal of the Electrochemical Society 151 (8) (2004) A1152–A1161.

[10] J. Lobato, P. Cañizares, M. Rodrigo, C. Ruiz-López, J. Linares, Influence of the Teflon loading in the gas diffusion layer of PBI-based PEM fuel cells, Journal of Applied Electrochemistry 38 (6) (2008) 793–802.

[11] M. Prasanna, H. Ha, E. Cho, S.-A. Hong, I.-H. Oh, Influence of cathode gas diffusion media on the performance of the PEMFCs, Journal of Power Sources 131 (1) (2004) 147–154.

[12] A. Tamayol, F. McGregor, M. Bahrami, Single phase through-plane permeability of carbon paper gas diffusion layers, Journal of Power Sources 204 (2012) 94–99.

[13] M. Ismail, T. Damjanovic, K. Hughes, D. Ingham, L. Ma, M. Pourkashanian, M. Rosli, Through-plane permeability for untreated and PTFE-treated gas diffusion layers in proton exchange membrane fuel cells, Journal of Fuel Cell Science and Technology 7 (5) (2010) 051016.

[14] J. M. LaManna, S. G. Kandlikar, Determination of effective water vapor diffusion coefficient in PEMFC gas diffusion layers, International Journal of Hydrogen Energy 36 (8) (2011) 5021–5029.

[15] N. Zamel, N. G. Astrath, X. Li, J. Shen, J. Zhou, F. B. Astrath, H. Wang, Z.-S. Liu, Experimental measurements of effective diffusion coefficient of oxygen–nitrogen mixture in PEM fuel cell diffusion media, Chemical Engineering Science 65 (2) (2010) 931–937.

[16] C. Chan, N. Zamel, X. Li, J. Shen, Experimental measurement of effective diffusion coefficient of gas diffusion layer/microporous layer in PEM fuel cells, Electrochimica Acta 65 (2012) 13–21.

[17] G. Hwang, A. Weber, Effective-Diffusivity Measurement of Partially-Saturated Fuel-Cell Gas-Diffusion Layers, Journal of The Electrochemical Society 159 (11) (2012) F683–F692.

[18] L. M. Pant, S. K. Mitra, M. Secanell, Absolute permeability and Knudsen diffusivity measurements in PEMFC gas diffusion layers and micro porous layers, Journal of Power Sources 206 (2012) 153–160.

[19] R. B. Bird, W. E. Stewart, E. N. Lightfoot, Transport Phenomena, Wiley, New York, 2 edn., 2002.

[20] M. M. Tomadakis, T. J. Robertson, Viscous permeability of random fiber structures: comparison of electrical and diffusional estimates with experimental and analytical results, Journal of Composite Materials 39 (2) (2005) 163–188.

[21] N. B. Carrigy, L. M. Pant, S. Mitra, M. Secanell, Knudsen Diffusivity and Permeability of PEMFC Microporous Coated Gas Diffusion Layers for Different Polytetrafluoroethylene Loadings, Journal of The Electrochemical Society 160 (2) (2013) F81–F89.

[22] D. Bruggeman, Calculation of various physics constants in heterogenous substances I Dielectricity constants and conductivity of mixed bodies from isotropic substances, Annalen der Physik 24 (7) (1935) 636–664.

[23] L. M. Pant, S. K. Mitra, M. Secanell, A generalized mathematical model to study gas transport in PEMFC porous media, International Journal of Heat and Mass Transfer 58 (1) (2013) 70–79.

Table 1: Thickness and Porosity (MIP) data of GDL samples

Sample	Thickness (μm)	Thickness after lamination (μm)	Porosity
SGL 34BA	260 ± 10	747±10 (3 layers)	0.77 ± 0.03
Toray090 (untreated)	273 ± 6	830±4 (3 layers)	0.76 ± 0.02
Toray090 (10% PTFE)	290 ± 4	874±19 (3 layers)	0.76 ± 0.01
Toray090 (20% PTFE)	283 ± 5	824±2 (3 layers)	0.69 ± 0.01
Toray090 (40% PTFE)	282 ± 4	814±16 (3 layers)	0.54 ± 0.01

Table 2: Through-plane permeability for sample SGL 34BA and Toray 090 (0, 10, 20 and 40% PTFE)

Sample	$B_v \times 10^{-11}$(m^2)	$B_l \times 10^{-5}$(m)	Literature ($B_v \times 10^{-11}$ (m^2))
SGL 34 BA	1.88 ± 0.46	0.26 ± 0.11	1.54 [21], 1.63 [5], 2.50 - 2.74 [18]
Toray 090 (0% PTFE)	0.80 ± 0.05	0.39 ± 0.11	1.10 [21], 0.90 [5]
Toray 090 (10% PTFE)	1.13 ± 0.12	0.51 ± 0.10	0.90 [21]
Toray 090 (20% PTFE)	0.66 ± 0.06	0.22 ± 0.04	0.73 [21]
Toray 090 (40% PTFE)	0.35 ± 0.12	0.05 ± 0.03	0.27 [21]

Table 3: Through-plane diffusibility for Toray 090 (0, 10, 20 and 40% PTFE)

Sample	Diffusibility	Literature (Toray 060 [16], Toray 120 [14, 15])
Toray 090 (0% PTFE)	0.209 ± 0.050	0.24-0.34 [16], 0.25-0.33 [15], 0.27-0.42 [14]
Toray 090 (10% PTFE)	0.193 ± 0.050	0.28-0.29 [15], 0.20-0.32 [14]
Toray 090 (20% PTFE)	0.144 ± 0.034	0.14-0.19 (30% PTFE) [16], 0.23-0.25 [15], 0.19-0.30 [14]
Toray 090 (40% PTFE)	0.071 ± 0.012	0.05 (60% PTFE) [16], 0.13-0.15 [15], 0.08-0.12 [14]

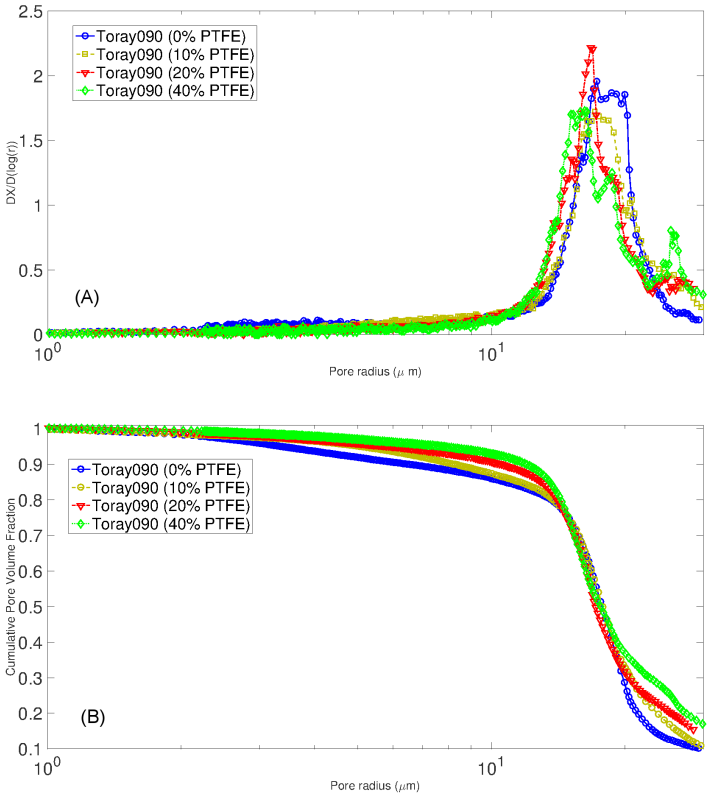

Figure 1: Pore size distribution of Toray 090 samples with different PTFE content (A) Logarithmic pore size distribution (B) Cumulative pore volume fraction distribution

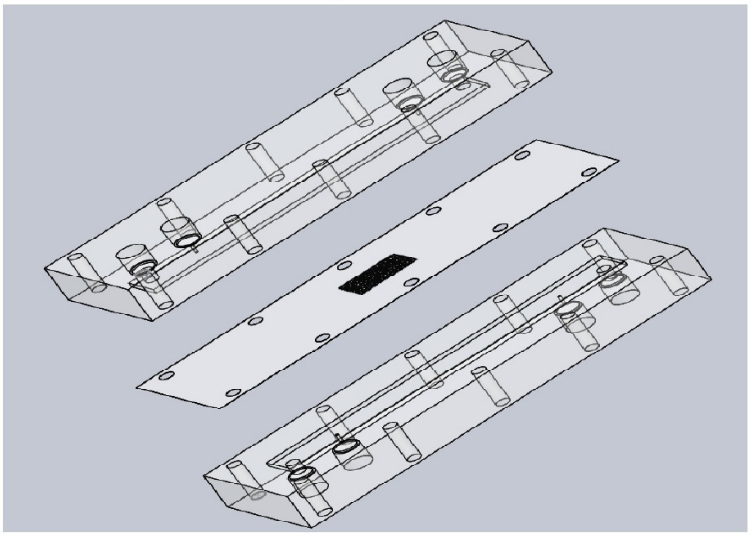

Figure 2: Exploded view of the through-plane diffusion bridge

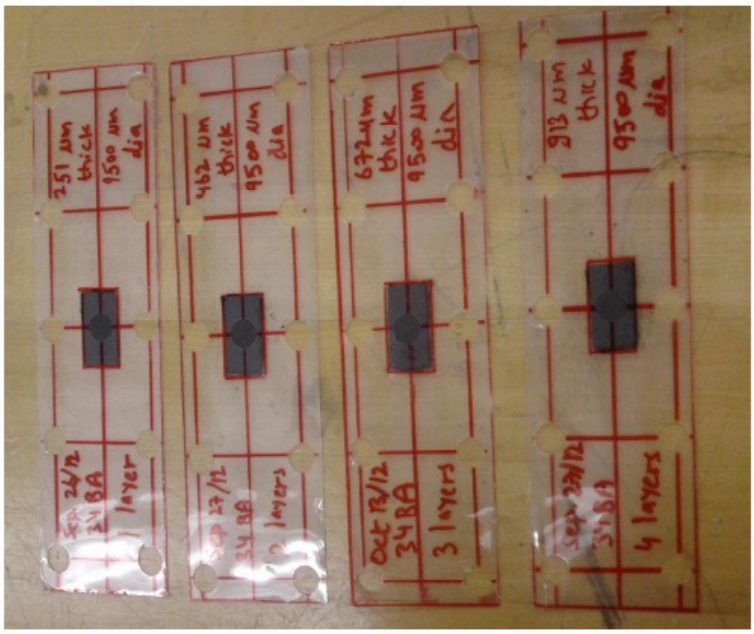

Figure 3: Laminated GDL samples

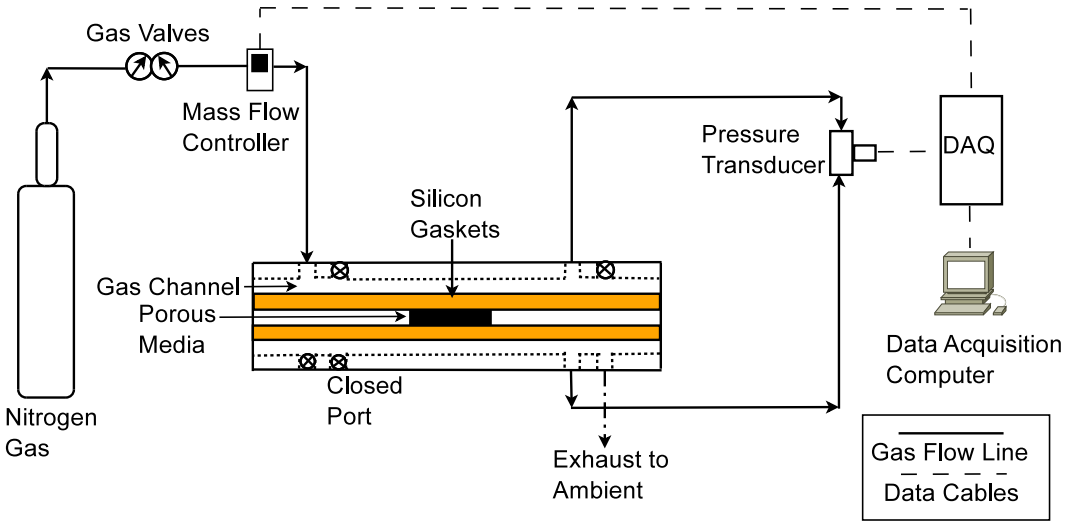

Figure 4: Schematic of the experimental setup to measure through-plane permeability

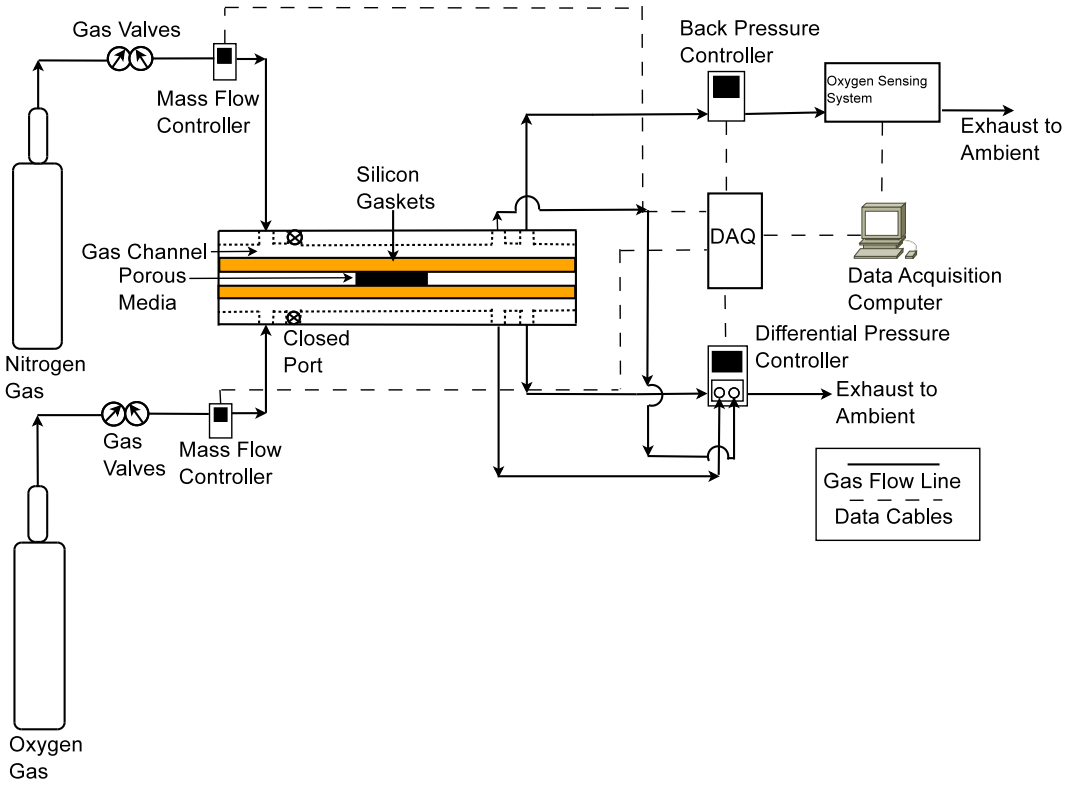

Figure 5: Schematic of the experimental setup to measure through-plane diffusivity

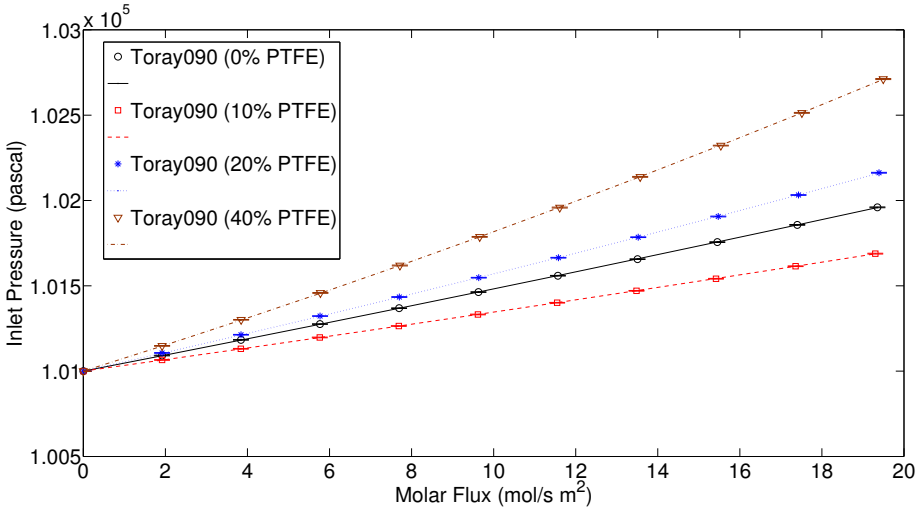

Figure 6: Inlet pressure vs molar flux for Toray 090 samples (error bars represent the standard deviation of the inlet pressure during a single experiment)

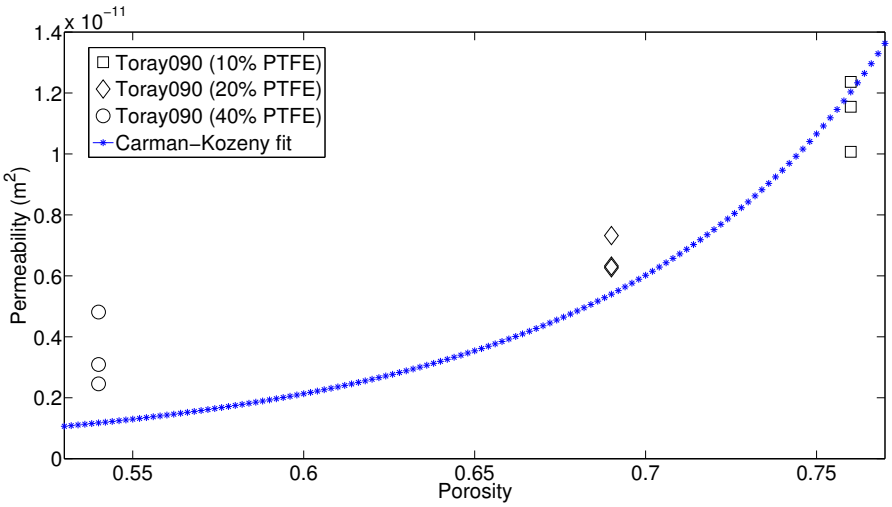

Figure 7: Carman-Kozeny fit to the experimental data (error bars obtained by testing 3 replicates of each sample)

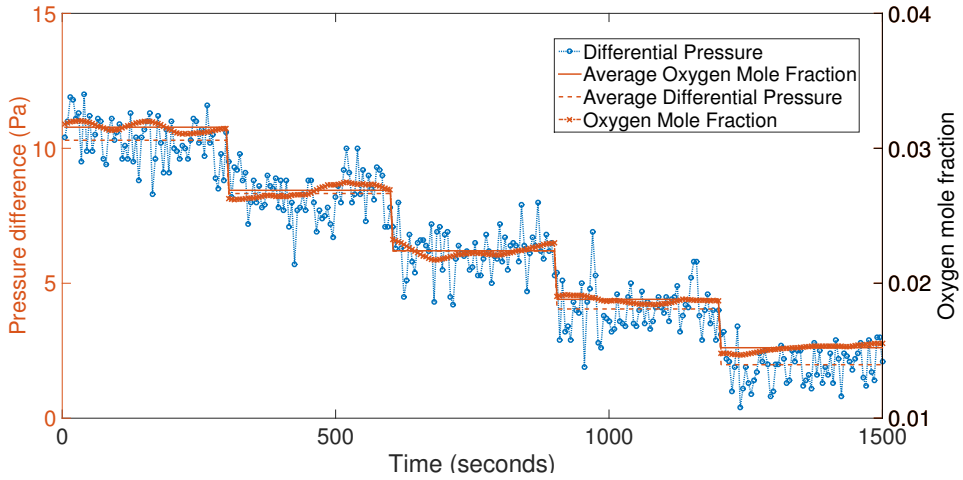

Figure 8: Oscillatory and average differential pressure, and oxygen concentration readings for a Toray 090 (10% PTFE) sample

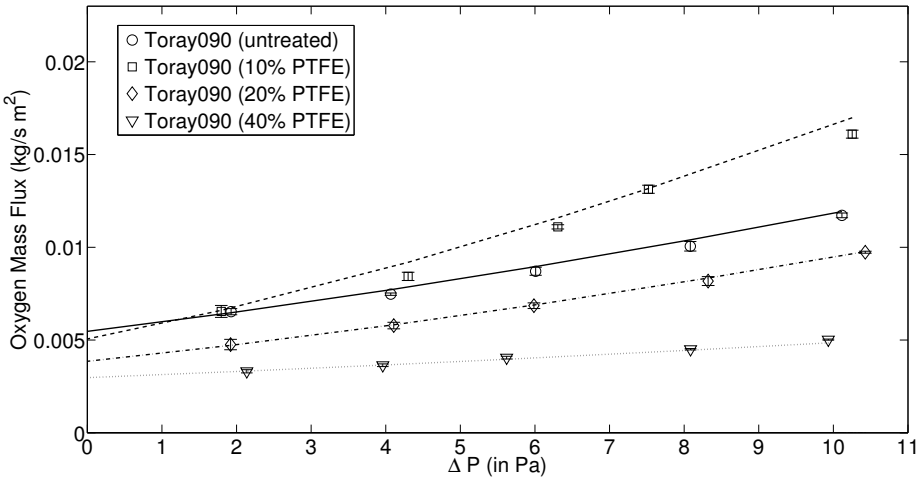

Figure 9: Oxygen mass flux vs differential pressure across porous media for GDL samples (error bars represent the standard deviation of the O_2 flux during a single experiment)

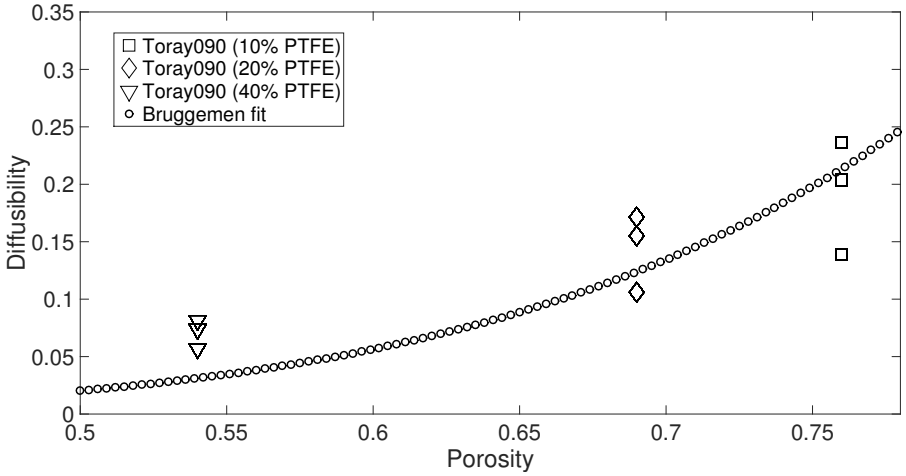

Figure 10: Bruggemen fit in diffusibility results (error bars obtained by testing 3 replicates of each sample)

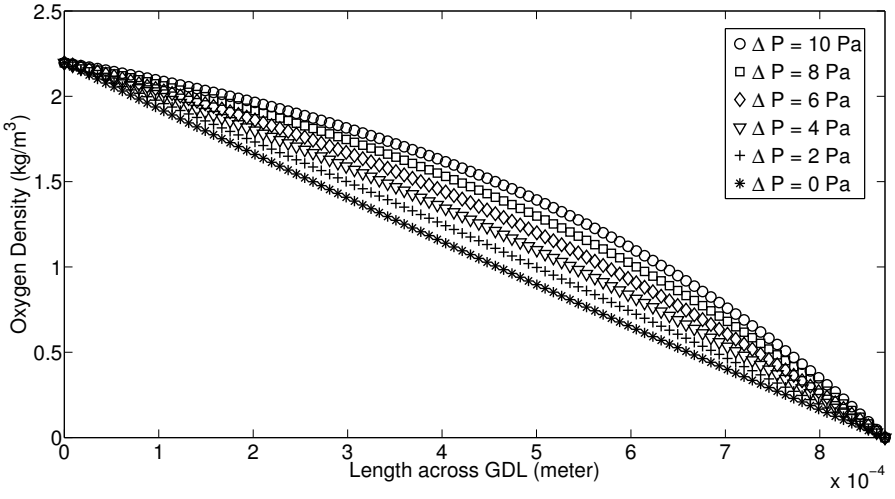

Figure 11: Oxygen density across porous media at various differential pressures

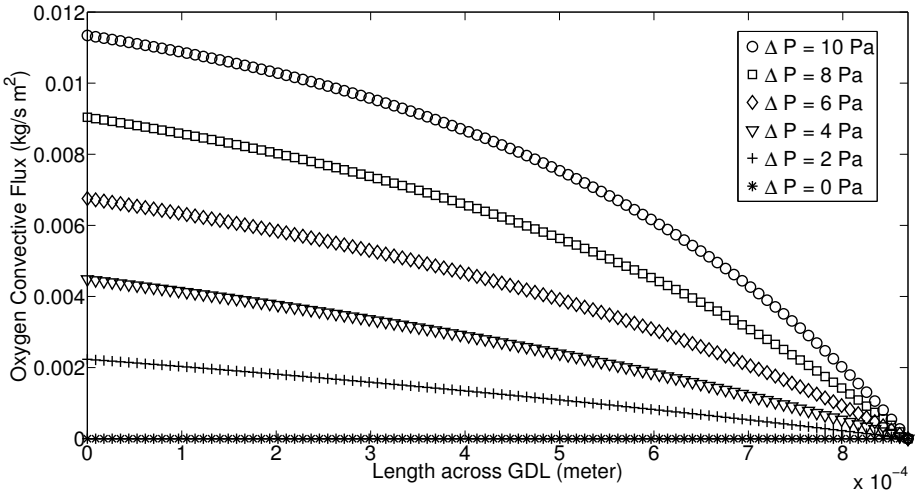

Figure 12: Oxygen convective flux across porous media at various differential pressures

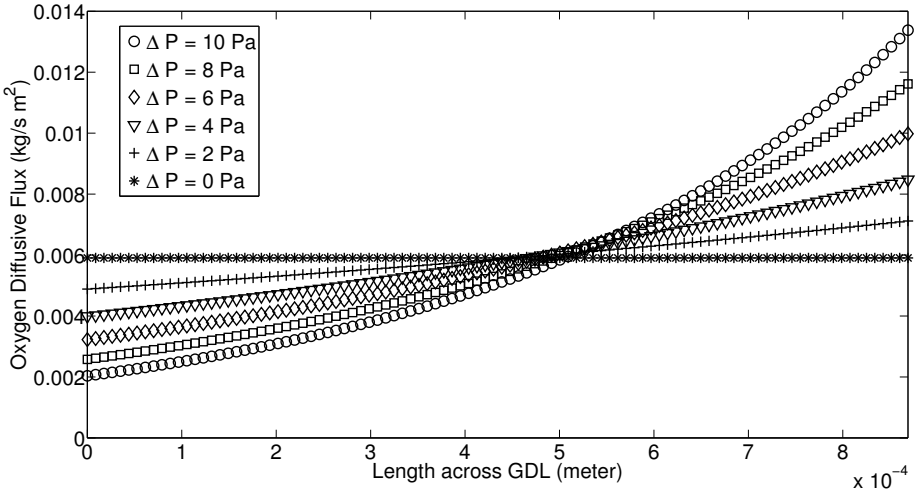

Figure 13: Oxygen diffusive flux across porous media at various differential pressures